

# Highly nonlinear solitary waves in chains of hollow spherical particles

Duc Ngo · Stephane Griffiths · Devvrath Khatri · Chiara Daraio

Received: 3 October 2011 / Published online: 30 January 2013  
© Springer-Verlag Berlin Heidelberg 2013

**Abstract** We study the dynamic response of one-dimensional granular chains composed of uniform hollow spheres excited by an impulse, and we observe the formation and propagation of highly nonlinear solitary waves. We find that the dynamics of these solitary waves are different from the solitary waves forming in chains composed of uniform solid spheres, because of the changes in the contact interaction between particles. We study the quasi-static contact interaction between two hollow spheres using finite element (FE) simulations, and approximate their response as a power-law type function in the range of forces of interest for this work. The experimental data obtained by testing a chain of particles shows good agreement with theoretical predictions obtained using a long wavelength approximation, and with numerical simulations based on discrete particle and FE models. We also investigate the effect of hollow spheres' wall thickness on the dynamic response of the chains.

**Keywords** Highly nonlinear solitary waves · Hollow spheres · Granular materials · Contact interaction

## 1 Introduction

The scientific community has shown an increasing interest in the dynamic response of granular chains (i.e., one-dimensional granular crystals), because of their characteristic, tunable dynamic behavior [1–20]. One-dimensional

homogenous chains of solid, elastic spheres represent the most commonly studied examples of granular crystals. These systems can exhibit linear, weakly nonlinear, and strongly nonlinear regime according to the precompression applied to the systems [1, 3, 4, 12]. In the strongly nonlinear regime (zero or very weak precompression compared to the amplitude of the dynamic excitations), it has been shown experimentally, analytically, and numerically [1, 2, 4, 5] that the systems, when excited by an impulse, support the formation and propagation of stable, highly nonlinear solitary waves. These waves are characterized by a compact shape with a finite spatial width ( $\sim 5$  particle diameters), and their propagation speed shows a nonlinear dependence on the wave amplitude, that is slow in comparison to the speed of sound in the material composing the particles in the chain [1, 2]. Such unique response originates from a double nonlinearity in the particles interaction: a power-law type contact potential in compression and a zero tensile strength. Another interesting characteristic of the systems is the tunability of their dynamic response. For example, in chains composed of solid spheres, it is possible to change the solitary waves' amplitude and traveling speed by changing the particle's dimension, material properties, and/or their periodicity [8, 12, 14, 15]. Recent studies on chains composed of ellipsoidal or cylindrical particles showed that the wave speed and amplitude can also be tuned by varying the particle geometry and the relative orientation between the particles [20, 21]. Based on these properties, granular crystals have been proposed for a variety of practical engineering applications, for example as shock absorbing materials [6, 11, 19, 22], in the generation of nonlinear waves for non-destructive evaluation of materials [23–26], and in sound focusing [27] or filtering [28] devices.

In this study, we focus on exploring the effects of the spherical particles' wall thickness on the formation and propagation of highly nonlinear solitary wave. We investigate

D. Ngo · S. Griffiths · D. Khatri · C. Daraio  
Graduate Aerospace Laboratories (GALCIT), California Institute of Technology, Pasadena, CA 91125, USA

C. Daraio (✉)  
Applied Physics, California Institute of Technology, Pasadena, CA 91125, USA  
e-mail: Daraio@caltech.edu

experimentally the propagation of highly nonlinear solitary waves in a one-dimensional chain composed of hollow spheres and compare the results with the theoretical predictions based on long wavelength approximation. We perform numerical simulations to study the response of the chain by using two independent approaches: discrete particle (DP) simulations and finite element (FE) simulations. The numerical results show good agreement with each other, and with the theoretical predictions and experimental observations.

The paper is organized as follows: In Sect. 2 we describe the experimental set up, in Sect. 3 we discuss the contact interaction between hollow spherical particles. Section 4 presents the long wavelength theory for highly nonlinear wave propagation adapted to a uniform chain of hollow spherical particles. Sections 5 and 6 describe the DP and FE models. In Sect. 7 we present a detail discussion and comparison of the results obtained. We end the paper with conclusions and considerations on their future applicability.

## 2 Experimental set-up and results

We performed our experiments on a one-dimensional chain composed of 29 hollow aluminum spheres placed horizontally on PTFE supporting rods as shown in Fig. 1a. These supporting rods ensured the unidirectional motion of the spheres along the chain's axis. The aluminum hollow spheres had an external diameter of  $D = 19.05$  mm and the wall-thickness was  $e_w = 0.87$  mm, which gives the outer radius of the sphere  $R_o = 9.525$  mm and the inner radius of the sphere  $R_i = 8.655$  mm. The ratio  $R_i/R_o$  of our hollow spheres was 0.91. The mass  $m_h$  of the particles was 2.38 g. The modulus of elasticity  $E$  of aluminum is 69 GPa and the Poisson ratio  $\nu$  is equal to 0.33 [29].

To monitor the wave propagation in the chain, we embedded piezoelectric sensors in instrumented particles in the chain. The instrumented sensors were custom fabricated in our lab by sandwiching a calibrated piezoelectric ring sensor (provided by Steiner & Martins, Inc., with an outer diameter of 19 mm, an inner diameter of 12 mm and a thickness of 0.75 mm) between two halves of a hollow sphere with glue (see Fig. 1b). These instrumented particles were pre-calibrated using conservation of momentum as described in [12], and they were placed in the 12th and the 19th positions respectively and connected to an oscilloscope (Tektronix TDS 2024) to measure the force amplitude and determine the wave speed in the chain. We generated the waves in the chain by impacting the chain with a hollow aluminum striker. The striker was launched from a ramp from different heights and the striker velocity was measured using an optical velocimeter.

After the striker had hit the chain, we observed a single wave propagating in the system (see Fig. 1c). The wave's

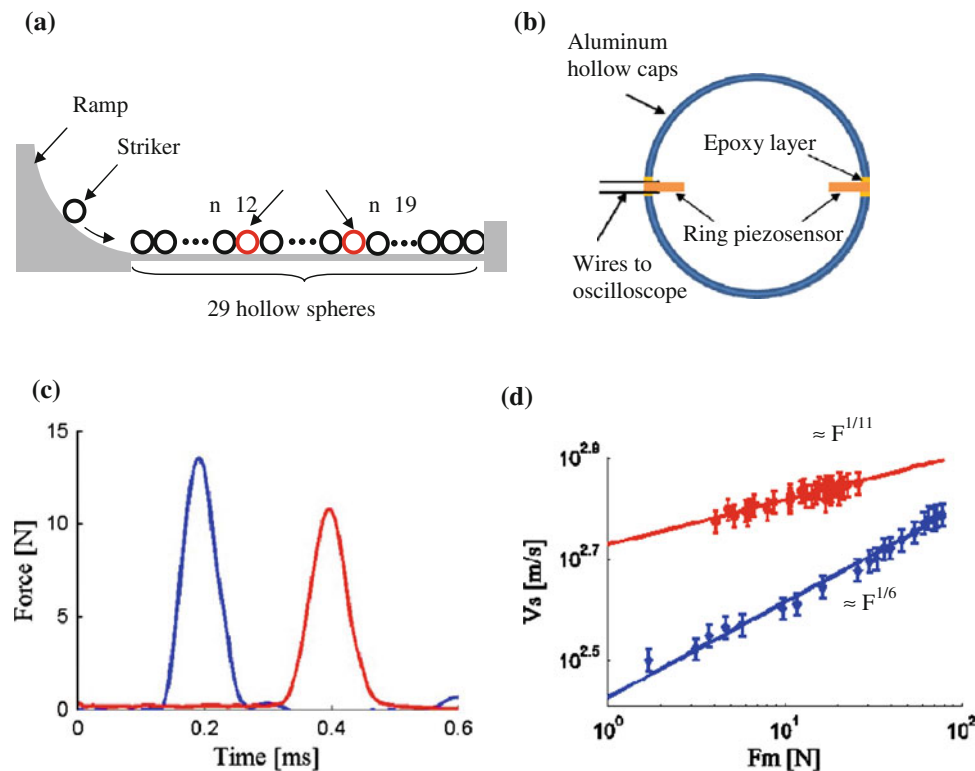
average propagating speed  $V_s$  was obtained by dividing the distance between two sensors by the time taken for the wave to travel from the first sensor to the second sensor. From the experimental velocity of the wave ( $V_s = 645$  m/s) and its temporal width, the characteristic spatial size  $L$  of the wave traveling in the chain was determined as  $L \approx 7.5 D$ . It should be noted that for a homogenous chain composed of solid aluminum spheres, in which the contact interaction between two consecutive particles follows the Hertzian contact's power law, the spatial width of the solitary wave propagating in the chain is approximately 5 particles [1].

Figure 1d presents the relation between the wave speed  $V_s$  propagating in the chain of hollow spheres and the average force amplitude  $F_m$  of the wave obtained from our experiments. The average force amplitude of the propagating waves was determined by taking the average of the force amplitudes detected at each sensor particles (i.e., particles number 12 and 19). We performed additional experiments on a chain composed of solid spheres to obtain its wave speed and force amplitude relation. The solid spheres used in experiments were solid aluminum spheres and had the same diameter as the hollow spheres. The mass of each solid sphere was  $m_s = 9.73$  g. The results of both the experiments are shown in Fig. 1d, with logarithmic scales are used in order to show the power-law dependence of the velocity to the force. Results reported in Fig. 1d show that different force amplitude-wave speed scalings are observed according to the properties of the spheres used in the chain. When the chain is composed of solid spheres, the speed of highly nonlinear solitary waves is proportional to the force amplitude to the power 1/6, as described in [1,4]. In the case of a chain made of hollow particles the speed of the highly nonlinear wave depends approximately on the force to the power 1/11 for the range of forces studied in this work. We did not observe any permanent deformation during experiments. The dynamic response of the systems is strongly affected by the geometry of the spheres, and the thickness of the wall may act on the propagation of the wave. The contribution of the wall's thickness to the dependence of the velocity to the force amplitude will be studied later in the paper using DP and FE simulations.

## 3 Contact interaction between hollow spherical particles

The contact interaction between two identical solid spheres under an applied compressive load was studied by Hertz [30]. In Hertz's study, the contact force  $F$  shows a power-law type dependence on the static overlap  $\delta$  between two spheres and is given by Hertz [30], Johnson [31]:

$$F = k_c \delta^{3/2} = \frac{2}{3} \sqrt{\frac{R}{2}} \frac{E}{(1-\nu^2)} \delta^{3/2}, \quad (1)$$



**Fig. 1** **a** Experimental setup used to measure the propagation of solitary waves in a chain composed of 29 hollow aluminum spheres. **b** Ring piezoelectric sensor embedded in a hollow aluminum bead. **c** Experimental results of a solitary wave propagation in the chain excited by impacting an identical hollow spherical striker of mass  $m = 2.38$  g with an impact velocity of 0.32 m/s the *blue curve* represents the results obtained at particle 12, the *red curve* represents the results obtained

at particle 19. **d** Comparison of experimental results for the relation between wave speed and force amplitude in logarithmic scales obtained from chains composed of solid and hollow aluminum spheres represented by *blue diamonds* and *red squares*, respectively. The *solid lines* correspond to linear fitting for both measurements (color figure online)

where  $k_c$  denotes the contact stiffness,  $R$  is sphere's radius, and  $E$  and  $\nu$  are the material's elastic modulus and Poisson ratio, respectively. The contact interaction between hollow spheres, especially for the case of very thin wall thickness, has been studied extensively. Updike and Kanin [32,33] provided a semi analytical approach to determine the compression force—displacement relation between a thin hollow hemisphere and a rigid plate, including also the buckling state of the thin wall. Pauchard and Rica [34] studied this problem experimentally and developed analytical formulas with not well-defined parameters to relate the elastic energy to displacement. More details about this topic can be found in Audoly and Pomeau [35]. However, a general closed-form formula for the contact interaction between two thin hollow spheres is not available.

In order to obtain the contact interaction response between the hollow spheres used in our experiments, we performed FE simulations. By taking advantages of the particle geometry, we constructed an axial symmetric FE model in Abaqus/CAE, and the model was solved by using Abaqus/

Standard. The FE model is shown in Fig. 2a with appropriate symmetry and boundary conditions. In this model, we used axisymmetric triangle elements (CAX6M) to mesh the particles. The material parameters of the particles such as density, modulus of elasticity, and Poisson's ratio used in FE simulations were obtained from the experimental setup described in Sect. 2. The contact interaction between two particles was modeled by using the standard surface-to-surface hard contact model of Abaqus/Standard. For simplicity, we modeled frictionless contact interaction in the tangential direction. More information regarding the Abaqus's elements and contact interaction can be found in [36].

To validate the accuracy of FE analysis, we first performed the FE simulations for the contact between solid spheres of same material and outer radius as our hollow spheres, and compared the results with Hertz's contact interaction [see Eq. (1)] as shown in Fig. 2b. It is evident that results obtained from FE simulations and Hertz's theory show an excellent agreement. We also perform FE simulations for different configurations of hollow spheres ( $R_i/R_o = 0.5, 0.75$ ) to study the effect of wall thickness on the contact interaction

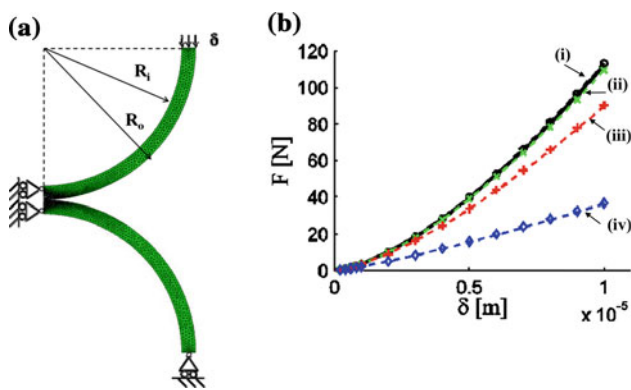


**Fig. 2** **a** Schematic diagram showing the axial symmetric FE model of two hollow spheres in contact with symmetry and boundary conditions. **b** Contact interactions obtained from FE simulations for selected values of  $R_i/R_o = 0$  (curve (i) in black),  $R_i/R_o = 0.5$  (curve (ii) in green),  $R_i/R_o = 0.75$  (curve (iii) in red),  $R_i/R_o = 0.91$  (curve (iv) in blue). The markers represent the FE results, the dashed curves are the power law fittings of the FE results. The *solid black curve* is obtained from the Hertzian contact interaction between two solid spheres of the same radius  $R_o$  (color figure online)

**Table 1** The values of the contact stiffness  $k$  and the exponent  $n$  obtained from FE simulations for selected values of  $R_i/R_o$

$R_i/R_o$	$k \times 10^9$	$n$
0	3.759	1.504
0.5	3.193	1.493
0.75	1.174	1.423
0.91	0.04671	1.222

between hollow spheres and the results are shown in Fig. 2b. Figure 2b shows clearly that the contact interaction between hollow spheres depends strongly on the wall thickness. As the wall thickness becomes thinner, the contact stiffness between two spheres decreases, as evident from the smaller slope of the force-displacement curves.

We approximate the contact interaction in the range of forces tested experimentally as a power law type function. The generalized contact interaction has the form:

$$F = k\delta^n. \quad (2)$$

Here the contact stiffness  $k$  and the exponent  $n$  depend on the ratio  $R_i/R_o$  and are obtained from fitting this power law to the FE results. The values of  $k$  and  $n$  we obtained are shown in Table 1 for different values of  $R_i/R_o$ . We find that, in the range of force considered in the experiments described in this paper, the power law fitting describes the relation between force and displacement. For a comparison, in the experiments done by Pauchard and Rica [33] for the contact between a tennis ball (with the ratio of  $R_i/R_o \approx 0.9$ ) and a rigid plate, the contact force was approximately proportional to the

displacement to the power 1.2, which is close to the value  $n = 1.222$  obtained from FE simulations for our hollow particles used in experiments.

#### 4 Solitary wave propagation in a chain of hollow sphere particles

To study analytically the propagation of highly nonlinear solitary waves in an uncompressed chain of solid spherical particles, Nesterenko [1] modeled the chain of spheres as a spring-mass system, where each particle is considered as point mass connected by nonlinear springs, defined by the power law Hertzian interaction [Eq. (1)]. From the discrete set of equations of motion for each particle of this system, using the long wavelength approximation, it is possible to derive the nonlinear partial differential wave equation that captures the characteristics of the system [1]. The solution of this equation describes compact solitary waves, with a wave speed  $V_s$  nonlinearly dependent on the maximum dynamic contact force (force amplitude)  $F_m$  in the chain [12] as:

$$\begin{aligned} V_s &= \frac{2}{\sqrt{5}} \left( \frac{k_c D^3}{m^{3/2}} \right)^{1/3} F_m^{1/6} \\ &= 0.682 \left[ \frac{2E}{D\rho^{3/2} (1-\nu^2)} \right]^{1/3} F_m^{1/6}. \end{aligned} \quad (3)$$

Nesterenko showed that systems characterized by a generalized power-law type contact interaction between particles also support the formation and propagation of highly nonlinear solitary waves [1]. Since, for predefined ranges of force, the contact interaction law for hollow spherical particles can be approximated by the power law type function as discussed in the previous section, uncompressed chains composed of hollow spherical particles are expected to support an analogous dynamic behavior to the chains of solid spheres. The analytical formulations describing the wave propagation in a chain of uniform hollow spheres can therefore be obtained following Nesterenko's approach [1]. Accordingly, the nonlinear relation between solitary wave speed  $V_s$  and force amplitude  $F_m$  in the chain of hollow spheres is given by Nesterenko [1]:

$$V_s = \sqrt{\frac{2}{n+1}} D \left( \frac{k^{1/n}}{m} \right)^{1/2} F_m^{\frac{n-1}{2n}}. \quad (4)$$

In the chain of hollow spheres used in our experiments, the wave speed is predicted to depend on the amplitude as  $V_s \sim (F_m)^{1/11}$  obtained from the value of exponent  $n = 1.222$ , showing a good agreement with the experimental data presented in Fig. 1d.

The width of the highly nonlinear solitary wave depends on exponent  $n$  as [1]:

$$L = \frac{\pi D}{n-1} \sqrt{\frac{n(n+1)}{6}}. \tag{5}$$

The exponent  $n = 1.222$  in the contact interaction of the hollow spheres used in experiments gives the width of the wave is around 9.5 times particles size, close to 7.5 particles size wave width observed in experiments.

### 5 Discrete particle simulations

We performed DP simulations to validate the analytical model and for comparison with the experimental results. Following previous studies [12, 14, 15], we modeled a chain composed of  $N$  uniform hollow spheres as a one-dimensional spring-mass system as described in the previous section. The equation of motion of the  $i$ th particle in the system is given by:

$$\ddot{u}_i = \frac{k}{m} [u_{i-1} - u_i]_+^n - \frac{k}{m} [u_i - u_{i+1}]_+^n, \tag{6}$$

where  $u_i$  is the displacement of the  $i$ th particle ( $i \in [1, \dots, N]$ ), and  $[x]_+$  denotes the positive part of  $x$ . The particle  $i = 0$  represented the striker. The value of the exponent  $n$  used in the DP simulations was obtained from the FE analysis as described in Sect. 3. We neglect the effect of dissipation. The numerical solutions of Eq. 6 was found by using the fourth order Runge–Kutta method. The time step of the integration used in the simulation was  $10^{-7}$ s, and the number of time steps simulated was 30,000. The error in the total energy of the system was in the order of  $10^{-8}$ .

### 6 Finite element simulations

We performed FE simulations to study the dynamic response of the chain composed of hollow spheres. We modeled a chain of 29 uniform hollow spheres and an identical striker using a FE model generated in Abaqus/CAE and it was solved in Abaqus/Explicit. The hollow-spherical particles were modeled as solid (continuum) axial symmetric two dimensional bodies, and they were meshed with triangular elements of second order. The appropriate mesh size for the particles was determined based on a mesh convergence study. The material and geometrical parameters of the hollow-spherical particles were obtained from the experimental setup. In Abaqus-Explicit, the contact interaction between any two particles was defined using surface-to-surface hard contact interaction.

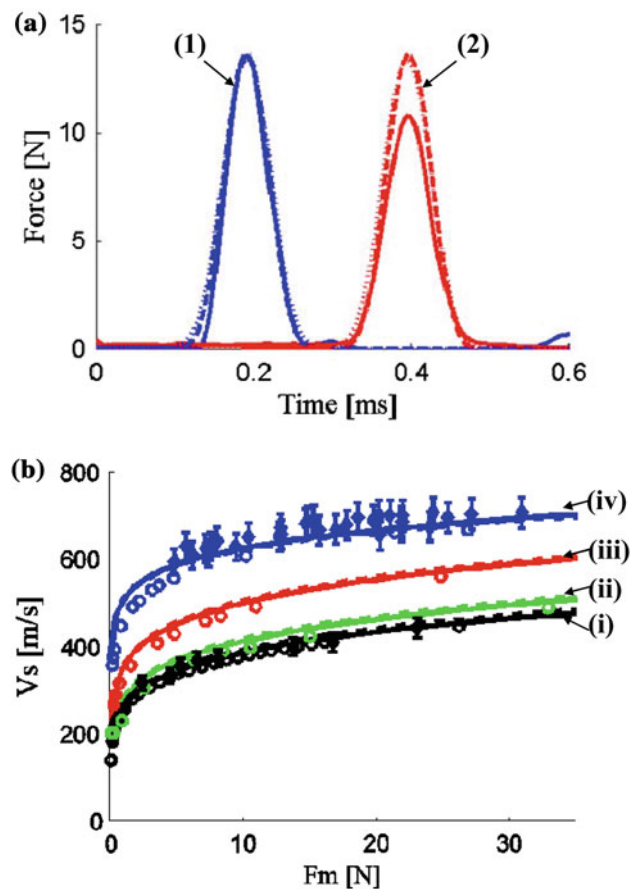


**Fig. 3** a Comparison of experimental and numerical results, obtained from DP and FE simulations, for the wave propagation in a chain of hollow spheres with  $R_i/R_o = 0.91$ . The curve group (1) in blue represents the results obtained at particle 12, the curve group (2) in red represents the results obtained at particle 19. The solid curves represent experimental data. The dashed curves are obtained from FE simulations, and the dotted curves from DP simulations. b Dependence of solitary wave speed on the dynamic force amplitude in the chain of hollow spheres when  $R_i/R_o = 0$  (curve group (i) in black), when  $R_i/R_o = 0.5$  (curve group (ii) in green), when  $R_i/R_o = 0.75$  (curve group (iii) in red), when  $R_i/R_o = 0.91$  (curve group (iv) in blue). Experimental data are reported only for  $R_i/R_o = 0.91$ , and they are shown by solid diamonds. The theoretical results in each group are represented by solid curves. The results obtained with our DP model are represented by dashed curves and the FEs results are represented by circles (color figure online)

### 7 Results and discussions

The wave propagation profiles obtained when the chain of 29 hollow spheres was excited by a striker with an impact velocity of 0.32 m/s is shown in Fig. 3a. We compared force-time responses measured by the instrumented particles in experiments, with the corresponding forces obtained from the DP and FE simulations, finding a good agreement. The presence of dissipation in the experimental data is noticeable by comparing the wave amplitude in particle 12 and particle 19. The solitary wave speed obtained

from the DP simulation was 648.5 m/s, from the FE simulation was 642.2 m/s, and from the experimental data was  $644.7 \pm 32.2$  m/s.

We also compared the relation between the solitary wave speed ( $V_s$ ) and the dynamic force amplitude ( $F_m$ ) in the chain of hollow spheres obtained from the experimental results, the theoretical predictions, and the numerical results (Fig. 3b). We found a good agreement between them, showing that chains of hollow spheres support robust formation of highly nonlinear solitary waves. This agreement also confirms the validity of the power law approximation for the contact interaction between hollow spheres in studying the dynamic response of chains of hollow spheres.

In Sect. 3, we showed that the variation in wall thickness of the hollow spheres affects significantly the contact interaction between them. We also investigated the effects of the wall thickness on the dynamic response of chains of hollow spheres. We performed numerical simulations and theoretical analysis to obtain the relations between the wave's speed and amplitude for selected values of  $R_i/R_o = 0, 0.5, 0.75, 0.91$ . The results were found to be in good agreement, as shown in Fig. 3b. It is important to notice that as the wall thickness increases, the systems support higher wave speeds for the same dynamic loading. The spatial width of the solitary waves is also observed to decrease as the wall thickness increases. This interesting dynamic tunability of the chains of hollow spheres can be found useful in some applications, such as in the design of tunable acoustic devices, or new impact protection systems.

## 8 Conclusions

The wave propagation in a one-dimensional chain composed of hollow spheres was studied using experimental, theoretical, and numerical approaches (DP and FE simulations). The contact interaction between two hollow spheres was characterized using FE simulations, and approximated by a power-law type interaction. We used this contact interaction to develop theoretical analysis of the wave propagation in the chain using a long wavelength approximation. We showed that this system supports the formation and propagation of highly nonlinear solitary waves; and we found good agreement between experiments, theory, and the numerical analyses. We also showed the effect of wall thickness on the wave propagation in the chains, which can be utilized to tune the stress propagation in granular chains.

**Acknowledgments** Support for this work was received from the Army Research Office (MURI grant US ARO W911NF-09-1-0436), and the National Science Foundation (NSF/CMMI-844540-CAREER and NSF/CMMI 0825345).

## References

1. Nesterenko, V.F.: Dynamics of Heterogeneous Materials. Springer, New York (2001)
2. Nesterenko, V.F.: Propagation of nonlinear compression pulses in granular media. *J. Appl. Mech. Tech. Phys.* **24**, 733 (1984)
3. Sen, S., Hong, J., Bang, J., Avalosa, E., Doney, R.: Solitary waves in the granular chain. *Phys. Rep.* **462**, 21–66 (2008)
4. Coste, C., Falcon, E., Fauve, S.: Solitary waves in a chain of beads under Hertz contact. *Phys. Rev. E* **56**, 6104–6117 (1997)
5. Chatterjee, A.: Asymptotic solution for solitary waves in a chain of elastic spheres. *Phys. Rev. E* **59**, 5912–5919 (1999)
6. Hong, J.: Universal power-law decay of the impulse energy in granular protector. *Phys. Rev. Lett.* **94**, 108001 (2005)
7. Job, S., Melo, F., Sokolow, A., Sen, S.: How solitary waves interact with boundaries in a 1d granular medium. *Phys. Rev. Lett.* **94**, 178002 (2005)
8. Daraio, C., Nesterenko, V.F., Herbold, E.B., Jin, S.: Strongly nonlinear waves in a chain of Teflon beads. *Phys. Rev. E* **72**, 016603 (2005)
9. Nesterenko, V.F., Daraio, C., Herbold, E.B., Jin, S.: Anomalous wave reflection at the interface of two strongly nonlinear granular media. *Phys. Rev. Lett.* **95**, 158702 (2005)
10. Vergara, L.: Delayed scattering of solitary waves from interfaces in a granular container. *Phys. Rev. E* **73**, 066623 (2006)
11. Doney, R., Sen, S.: Decorated, tapered, and highly nonlinear granular chain. *Phys. Rev. Lett.* **97**, 155502 (2006)
12. Daraio, C., Nesterenko, V.F., Herbold, E.B., Jin, S.: Tunability of solitary wave properties in one dimensional strongly nonlinear phononic crystal. *Phys. Rev. E* **73**, 026610 (2006)
13. Job, S., Melo, F., Solokow, A., Sen, S.: Solitary wave trains in granular chains: experiments, theory and simulations. *Granul. Matter* **10**, 13–20 (2007)
14. Porter, M.A., Daraio, C., Herbold, E.B., Szelengowicz, I., Kevrekidis, P.G.: Highly nonlinear solitary waves in phononic crystal dimers. *Phys. Rev. E* **77**, 015601 (2008)
15. Porter, M.A., Daraio, C., Herbold, E.B., Szelengowicz, I., Kevrekidis, P.G.: Highly nonlinear solitary waves in heterogeneous periodic granular media. *Phys. D* **238**, 666–676 (2009)
16. Carretero-Gonzalez, R., Khatri, D., Porter, M.A., Kevrekidis, P.G., Daraio, C.: Dissipative solitary waves in periodic granular media. *Phys. Rev. Lett.* **102**, 024102 (2009)
17. Harbola, U., Rosas, A., Romero, A.H., Esposito, M., Lindenberg, K.: Pulse propagation in decorated granular chains: an analytical approach. *Phys. Rev. E* **80**, 051302 (2009)
18. Molinari, A., Daraio, C.: Stationary shocks in elastic highly nonlinear granular chains. *Phys. Rev. E* **80**, 056602 (2009)
19. Daraio, C., Nesterenko, V.F., Herbold, E.B., Jin, S.: Energy trapping and shock disintegration in a composite granular medium. *Phys. Rev. Lett.* **96**, 058002 (2006)
20. Ngo, D., Khatri, D., Daraio, C.: Solitary waves in uniform chains of ellipsoidal particles. *Phys. Rev. E* (2011) (in press)
21. Khatri, D., Ngo, D., Daraio, C.: Solitary waves in uniform chains of cylindrical particles. *Granul. Matter* (2011). (accepted)
22. Fraternali, F., Porter, M.A., Daraio, C.: Optimal design of composite granular protectors. *Mech. Adv. Mat. Struct.* **17**, 1–19 (2010)
23. Sen, S., Manciu, M., Wright, J.D.: Solitonlike pulses in perturbed and driven Hertzian chains and their possible applications in detecting buried impurities. *Phys. Rev. E* **57**, 2386–2397 (1998)
24. Hong, J., Xu, A.: Nondestructive identification of impurities in granular medium. *Appl. Phys. Lett.* **81**, 4868–4870 (2002)
25. Khatri, D., Daraio, C., Rizzo, P.: Highly nonlinear waves' sensor technology for highway infra structure. In: SPIE Smart Structures/NDE, 15th Annual International Symposium, San Diego, Manuscript number 6934–25 (2008).

26. Yang, J., Silvestro, C., Khatri, D., Nardo, L.D., Daraio, C.: Interaction of highly nonlinear solitary waves with linear elastic media. *Phys. Rev. E* **83**, 046606 (2011)
27. Spadoni, A., Daraio, C.: Generation and control of sound bullets with a nonlinear acoustic lens. *Proc. Natl. Acad. Sci. USA* **107**, 7230 (2010)
28. Boechler, N., Theocharis, G., Daraio, C.: Bifurcation based acoustic switching and rectification. *Nat. Mater.* (2011) (Published Online)
29. <http://www.efunda.com>, <http://mat.web.com>
30. Hertz, H.: On the contact of rigid elastic solids. *J. Reine Angew. Math.* **92**, 156 (1881)
31. Johnson, K.L.: *Contact Mechanics*. Cambridge University Press, Cambridge (1985)
32. Updike, D.P., Kalnins, A.: Axisymmetric behavior of an elastic spherical shell compressed between rigid plates. *J. Appl. Mech.* **37**, 635 (1970)
33. Updike, D.P., Kalnins, A.: Axisymmetric postbuckling and non-symmetric buckling of a spherical shell compressed between rigid plates. *J. Appl. Mech.* **39**, 172 (1972)
34. Pauchard, L., Rica, S.: Contact and compression of elastic spherical shells: the physics of a 'ping-pong' ball. *Philos. Mag. B* **78**, 225–233 (1998)
35. Audoly, B., Pomeau, Y.: *Elasticity and Geometry: From Hair Curls to the Nonlinear Response of Shells*. Oxford University Press, Oxford (2010)
36. Simulia, Abaqus version 6.8 Documentation, D.S.S.A., (ed.). Providence (2008)